

Microscopic superconducting parameters from tunneling in A_{15} Nb-Sn

D. A. Rudman*

Department of Physics, Stanford University, Stanford, California 94305

M. R. Beasley

Departments of Applied Physics and Electrical Engineering, Stanford University, Stanford, California 94305

(Received 16 March 1984)

High-quality tunnel junctions have been fabricated on thin films of A_{15} Nb-Sn (20–25 at. %) using oxidized a -Si tunnel barriers and Pb counterelectrodes. These junctions have been used to measure changes in the gap, the transition temperature T_c , and the tunneling density of states with composition in this important high- T_c superconductor. With the use of the proximity-effect-modified data reduction scheme developed by Arnold and Wolf, values for $\alpha^2F(\omega)$ and μ^* are obtained. As the Sn content approaches stoichiometry, the lowest-energy phonon branch in $\alpha^2F(\omega)$ both increases in weight and shifts to lower energy. These two effects combine to produce the increases in λ as stoichiometry is approached, and at the same time can account for the observed increase in $2\Delta/k_B T_c$. The values of μ^* remain essentially constant as a function of composition, and hence show no evidence for an increased Coulomb interaction with increasing disorder as recently proposed by Anderson *et al.*

I. INTRODUCTION

The superconducting properties of the high- T_c A_{15} compounds are in general a strong function of composition, with both the critical temperature T_c and the energy gap Δ increasing rapidly as either stoichiometry or the A_{15} phase boundary is approached.^{1–5} The origins of these changes can be investigated using electron tunneling spectroscopy as a probe of the microscopic superconducting parameters of these materials.⁶ However, until recently tunneling studies on A_{15} transition-metal compounds have not been successful due to the difficulty in obtaining high-quality tunnel junctions on well-controlled samples.

This situation has been greatly improved by the use of vapor deposition techniques to fabricate uniform thin-film samples, and the success of thin oxidized overlayers as artificial tunneling barriers. Junctions made using these techniques have been of sufficiently high quality to perform quantitative tunneling studies on Nb-Al (Ref. 2) and Nb-Ge (Ref. 3). In this paper we report on the results of a systematic study of the superconducting properties of the A_{15} Nb-Sn system (20–25 at. % Sn). These data represent the culmination of our tunneling study of the Nb-Sn system begun by Moore and co-workers.^{1,7}

II. SAMPLE PREPARATION

The samples used in this study were deposited onto heated ($\sim 800^\circ\text{C}$) single-crystal sapphire substrates using the electron-beam codeposition system developed by Hammond.⁸ Samples covering the entire A_{15} composition range were made in a single deposition by using the gradient in composition inherent in evaporation from two separated sources. In a typical deposition, 500 nm of Nb-Sn are deposited at a rate of ~ 2 nm/sec in a vacuum (during deposition) of $\sim 1 \times 10^{-7}$ Torr. After cooling the

samples in vacuum, a thin (2–3 nm) overlayer of a -Si is deposited. Upon exposure to air (~ 24 h) this layer oxidizes to form a reliable tunneling barrier.⁹ The junction is completed with a Pb counterelectrode. Details of the deposition parameters necessary to form optimum material and high-quality junctions have been reported elsewhere.¹⁰ All the samples to be discussed in this paper are listed in Table I with their deposition conditions, composition, and inferred superconducting parameters. Table I has been organized by gap as this has proved to be the most consistent parameter for characterizing a sample's superconducting properties.

III. TUNNELING RESULTS

Figure 1 shows a series of current-voltage (I - V) characteristics typical of those used in this study. These junctions have very low leakage current at zero-voltage bias (typically $< 0.5\%$), indicating that the conduction is almost entirely by tunneling. There is some excess conduction (typically 4–9%) below the sum of the gaps, with an S - I - N -like (superconductor-insulator-normal-metal) onset at the Pb gap (1.3 mV).¹⁰ In all junctions studied the gap structure ($\Delta_{\text{Nb-Sn}} + \Delta_{\text{Pb}}$) is quite broad, so that the single gap value assigned each junction has been operationally defined as the inflection point in the I - V curve.

For each junction the critical temperature of the material being probed by tunneling (typically only the top 10 nm) can be determined by measuring the temperature at which all gap structure disappears from the zero-bias conductance, T_c^{gap} . (It has been found¹⁰ that T_c^{gap} is always within a few percent of the inductively measured transition for the sample, T_c^L .) However, the temperature dependence of the zero-bias conduction differs from the calculated behavior of an ideal junction in a manner which strongly suggests that the majority of the material

TABLE I. Important physical and superconducting parameters for samples in this study.

Sample no.	Δ (meV)	T_c^* (K)	T_c^{gap} (K)	Nominal at. % Sn ^a	Deposition temperature (°C)	$\rho(T_c)^b$ ($\mu\Omega$ cm)	λ	$\langle\omega^2\rangle$	$\mu^*(\omega_{\text{ph}})^c$
1	3.30	17.0	17.4	25.5	880	5.6	1.63	231	0.14
2	3.25	16.9	17.3	26.7	765	27	1.75	201	0.14
3	3.20	17.1	17.4	25.6	770	11	1.70	203	0.15
4	3.03	16.0	16.7	25.7	765	33	1.51	229	0.13
5	2.80	15.5	16.2	24.1	880	16	1.35	246	0.12
6	2.73	15.0	16.3	24.9	765	45	1.37	251	0.13
7	2.63	14.9	15.9	25.6	780	22	1.31	224	0.11
8	2.30	14.0	15.2	24.5	765	48	1.23	257	0.13
9	2.28	14.2	15.2	24.8	780	24	1.29	236	0.14
10	1.85	12.1	14.0	24.0	765	54	1.19	249	0.14
11	1.85	11.3	12.0	22.4	880	29	1.13	234	0.12
12	1.57	10.4	13.0	23.2	765	62	0.98	278	0.12
13	1.49	d	12.2	23.4	780	30	0.98	274	0.14

^aNominal Sn percentage are likely ≈ 1 at. % high. See Ref. 10.

^bResistivity just above T_c .

^c μ^* defined at the phonon cutoff frequency ω_{ph} , as in Ref. 27.

^dInsufficient data to calculate T_c^* .

sampled by the tunneling electrons has gone normal (or gapless) at a temperature T_c^* lower than T_c^{gap} .^{10,11}

Figure 2 shows T_c^* as a function of gap for the samples used in this study. For a given gap value, T_c^* is found to be insensitive to the deposition conditions used to make the Nb-Sn. In contrast, T_c^{gap} varies over a wide range for the same samples, as shown by the shaded region in Fig. 2. Note that T_c^{gap} falls outside the BCS weak-coupling limit for the low-gap material, corresponding to values of $2\Delta/k_B T_c^{\text{gap}}$ below the BCS limit. (A similar depression of $2\Delta/k_B T_c$ below the BCS limit has been observed in other A15 superconducting compounds.^{2,3}) In Nb-Sn this problem does not occur if T_c^* is chosen as the appropriate transition temperature for the gap value of the junction. The difference between T_c^* and T_c^{gap} may simply reflect

imperfections at the surface of the material. However, heat-capacity measurements on similar samples show a broadened bulk transition as well.¹² The origin of this problem in Nb-Sn and other high- T_c A15 compounds is not fully understood and is currently under investigation.¹³

To obtain information about the microscopic superconducting parameters in this material, the differential conductance $\sigma(V) = (dV/dI)^{-1}$ was measured for each junction using a standard harmonic-detection technique.¹⁴ The superconducting-state conductance $\sigma_S(V)$ (at $T = 1.4$ K) of the Nb-Sn was measured with the Pb counterelectrode driven normal by an applied field (~ 0.1 T), and the

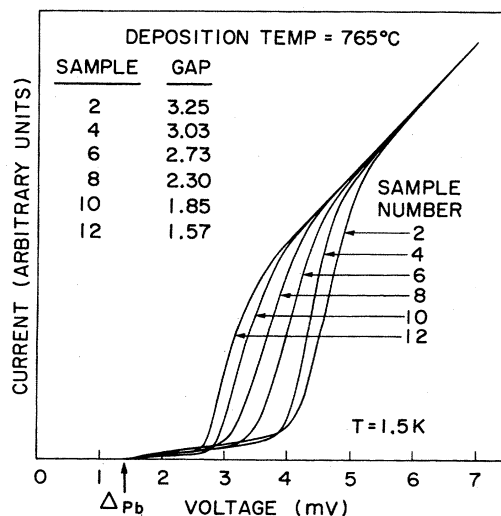


FIG. 1. Current-voltage characteristics for samples from one deposition. Sample numbers refer to Table I.

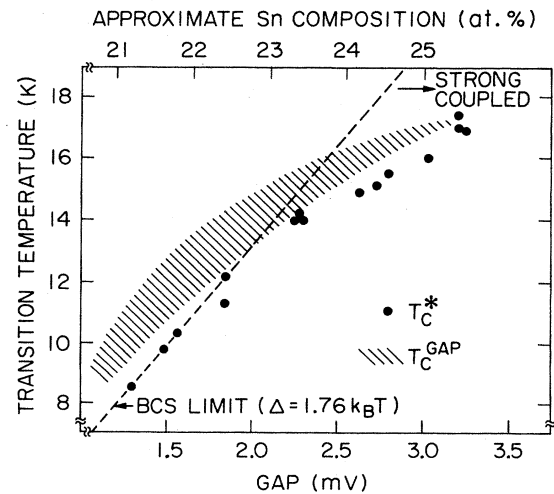


FIG. 2. Dependence of the junction transition temperature T_c^* on the gap. Shaded area represents the range of values obtained for T_c^{gap} (the maximum T_c) for the same samples. Dashed line is the BCS limit $\Delta = 1.76 k_B T_c$.

normal-state conductance $\sigma_N(V)$ measured by raising the temperature above T_c (Nb-Sn). The tunneling conductance

$$\sigma_T(V) = \frac{\sigma_S(V)}{\sigma_N(V)}$$

was corrected for the small excess conductance found below the gap, and then used as the tunneling density of states (TDOS) in the McMillan-Rowell (MR) program¹⁵ for inverting the Eliashberg equations to obtain the electron-phonon coupling spectrum $\alpha^2F(\omega)$ and the renormalized Coulomb potential μ^* .

The results from the MR program have several anomalies. As shown by the dashed line in Fig. 3 for a stoichiometric sample, the MR-calculated TDOS (plotted as the deviation from the BCS density of states) deviates strongly from the experimental curve (solid line) in overall magnitude and shape at high energies. The resulting $\alpha^2F(\omega)$ is much smaller in magnitude than expected, and typically μ^* must be made negative to reproduce the measured gap. Finally, the calculated phonon cutoff energy does not agree with the measured value.

All of these anomalous features have been found previously in transition-metal tunneling results, including Nb₃Sn.^{1,7,16,17} To explain these features, Arnold¹⁸ suggested the presence of a thin normal layer at the surface of the superconductor, corresponding to an SN-I-N' (superconductor/normal-insulator-normal-metal) proximity effect tunnel junction. Wolf *et al.*¹⁷ showed that intentionally made SN-I-N' junctions reproduce all the above features and that a modified McMillan-Rowell (MMR) program can be used to extract corrected $\alpha^2F(\omega)$ and μ^* . The modified program introduces two new parameters to account for the normal layer.¹⁹

Owing to the similarities between our tunneling density of states and those found by Wolf and Arnold, and because of the tendency of the A15 superconductors to be either A-element or B-element rich at the surface when slightly oxidized,²⁰ we have used the MMR-data reduction scheme for our Nb-Sn junctions. Since the origin and na-

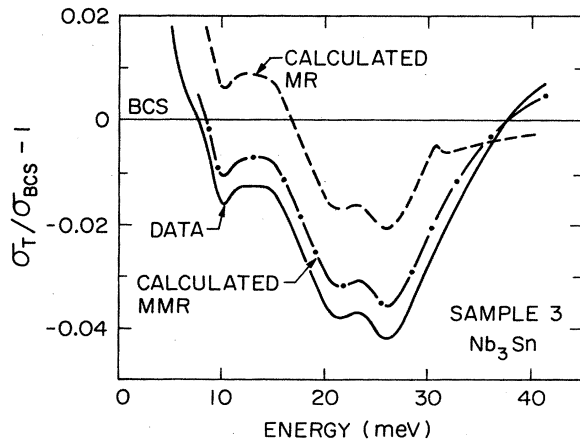


FIG. 3. Comparison of the experimental tunneling density of states (plotted as the deviation from the BCS density of states) to the calculated TDOS obtained from the standard (MR) and proximity-modified (MMR) inversion analyses. Proximity parameters used were $R=7.0$ (μeV) and $d/1=0.060$ (see Ref. 19).

ture of this proximity layer is unknown for our samples, we use the two proximity-effect parameters as fitting parameters to minimize the difference between the experimental and calculated TDOS. In this fitting we also use the constraints that the calculated TDOS correctly reproduce the observed cutoff energy and phonon peak locations as determined experimentally from $d\sigma_S(V)/dV$.¹⁵

The use of the MMR procedure greatly improves the agreement between the calculated (dotted-dashed line in Fig. 3) and the experimental TDOS, although there is still a deviation of $\sim 2\%$ with the "best fit." While the proximity parameters (as well as the value chosen for the gap) affect the overall magnitude of $\alpha^2F(\omega)$, both the shape of $\alpha^2F(\omega)$ and the location of the phonon peaks are quite insensitive to these parameters over a reasonable range of values. The effect of this procedure and the method used to select the proximity parameters are given elsewhere.¹¹

Figure 4 shows $\alpha^2F(\omega)$ spectra for three different compositions (and gaps) of Nb-Sn. The dashed curves at low energy show where the measured $\alpha^2F(\omega)$ have been replaced by a Debye-type spectrum ($\sim \omega^2$) due to the unreliability of the low-energy data.¹⁵ As the composition approaches stoichiometry, $\alpha^2F(\omega)$ undergoes two distinct changes. The overall strength of $\alpha^2F(\omega)$ increases, with a marked increase in the relative weight of the lowest-energy phonon branch. At the same time there is a monotonic decrease in the position (energy) of this lowest branch. These two factors combine to produce a large increase in the electron-phonon coupling constant

$$\lambda = 2 \int [d\omega \alpha^2F(\omega)/\omega],$$

and a corresponding decrease in the weighted average-phonon frequency. These changes are shown in Fig. 5, which plots λ and

$$\langle \omega^2 \rangle = (2/\lambda) \int d\omega \alpha^2F(\omega)\omega$$

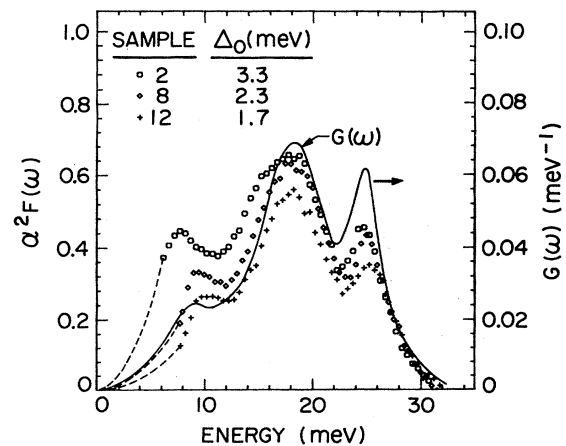


FIG. 4. Electron-phonon spectral function $\alpha^2F(\omega)$ for three samples representing the full range of gap values studied. Sample numbers refer to Table I. The Debye-type spectrum assumed at low energy is shown as the dashed lines. The solid line shows the phonon spectrum $G(\omega)$ obtained from neutron scattering (Ref. 23) for stoichiometric Nb₃Sn, normalized to the peak height of the stoichiometric tunneling sample.

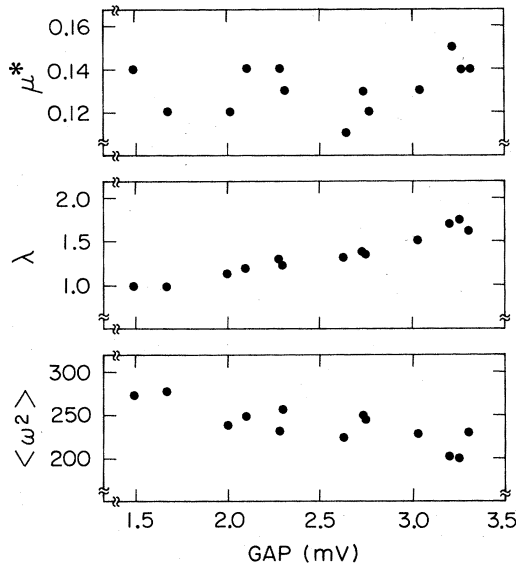


FIG. 5. The superconducting parameters μ^* , λ , and $\langle\omega^2\rangle$ derived from the MMR program plotted vs the gap for all samples in this study.

versus gap for all junctions studied. Also shown are the μ^* values obtained from the analysis.

IV. DISCUSSION

A shift of the lowest-energy phonon branch to lower energy, or “mode softening,” has also been previously found in the $A15$ compounds Nb-Al (Ref. 2) and Nb-Ge (Ref. 3), and may be a general property of the high- T_c Nb-based $A15$ superconductors. The importance of mode softening and the relative roles of the average phonon frequency and the electronic band density of states in these high- T_c materials have been discussed by Kwo *et al.*²¹ In the Nb-Sn system the band density of states has been previously found (from the critical field²²) to increase by about 25% as stoichiometry is approached. In this work we have found that $\langle\omega^2\rangle$ decreases by about the same amount. Thus from the point of view of the analysis of Kwo *et al.*, for Nb-Sn both of these factors are needed to account for the observed increase in λ and the corresponding increase in T_c with composition.

The observed increase in the overall strength of $\alpha^2F(\omega)$ with increasing Sn concentration probably represents an enhancement of the electron-phonon coupling constant α^2 [since $F(\omega)$ is a normalized quantity]. In addition, the relative increase in the weight of the lowest-energy phonon branch suggests that the change in $\alpha^2(\omega)$ is not energy independent, but is largest at low energies.

For stoichiometric Nb₃Sn it is possible to compare $\alpha^2F(\omega)$ to the generalized phonon distribution function $G(\omega)$ obtained from inelastic neutron scattering on a powdered sample²³ as shown by the solid line in Fig. 4. In Fig. 4 $G(\omega)$ has been scaled to match the maximum height of the stoichiometric tunneling sample. The two spectra agree well in phonon peak location and cutoff energy, although the lowest-energy branch occurs at a

slightly lower energy in the tunneling sample than in the neutron data sample. The relative intensities of the peak heights suggest that $\alpha^2(\omega)$ is a monotonically decreasing function of energy, as proposed by Appel and Kohn²⁴ for transition-metal alloys.

The effects of changes in the relative weighting of $\alpha^2F(\omega)$ on T_c and gap have been calculated as functional derivatives by other workers. Bergmann and Rainer²⁵ found that T_c is most sensitive to increases in $\alpha^2F(\omega)$ at $\omega=8k_B T_c$ (~ 12 meV for Nb₃Sn), while Mitrovic *et al.*²⁶ found that Δ is most sensitive at half this energy, or $\omega=4k_B T_c$. Thus for Nb-Sn the increases in the lowest-energy phonon branch ($\omega=8-10$ meV) occur at nearly the optimal energy to enhance both T_c and Δ , while the mode softening near stoichiometry changes $\alpha^2F(\omega)$ in such a way as to increase Δ relative to T_c , as is observed in the increase in $2\Delta/k_B T_c$ with Sn concentration.

Finally, the inversion of the Eliashberg equations also produces values for the renormalized Coulomb potential μ^* . Unfortunately, μ^* is most sensitive to the low-energy values of the TDOS. Since these values are very difficult to measure accurately, the resulting μ^* in general have also been considered not fully reliable. However, it is possible to check the self-consistency of the proximity-effect modified solution by using the $\alpha^2F(\omega)$ and μ^* to calculate T_c^{calc} from the Eliashberg equations. The value of μ^* found by the MMR program is scaled to the (arbitrary) cutoff energy chosen for the integration, and must be rescaled as described by Allen and Dynes²⁷ to perform this calculation. Once this is done, the resulting values of T_c^{calc} agree to within better than 2% with the value T_c^* (not T_c^{gap}) measured for the sample. While the calculation of the correct T_c does not confirm the appropriateness of the proximity-effect model, it does at least indicate that the modifications have not disrupted the self-consistent nature of the solution. Moreover, the very close agreement between T_c^{calc} and T_c^* supports the identification of T_c^* as the appropriate critical temperature for the gap value assigned the junction.

While the exact reliability of these μ^* values is not known, qualitatively it is seen (Fig. 5) that μ^* remains essentially constant for all samples in this study. In particular, there is no evidence for a large increase in μ^* with resistivity (disorder), as has been proposed by Anderson *et al.*,²⁸ to explain the “universal” degradation of T_c with resistivity in this class of materials. Instead, the observed decrease in λ is sufficient to account for the decrease in T_c . Whether this result reflects a failure of strong-coupling theory to interpret the data for these high-resistivity materials is not known. It is hoped that the availability of detailed information about the microscopic superconducting parameters such as given here will allow more careful testing of the current theories of these premier high- T_c superconducting materials.

ACKNOWLEDGMENTS

We would like to thank R. H. Hammond and F. Hellman for valuable help in the sample preparation phase of this project, and J. Kwo and K. Kihlstrom for help with the data analysis. This work was supported by the Office of Naval Research, U.S. Department of the Navy.

- *Present address: Department of Materials Science and Engineering, Massachusetts Institute of Technology, Cambridge, MA 02139.
- ¹D. F. Moore, R. B. Zubeck, J. M. Rowell, and M. R. Beasley, *Phys. Rev. B* **20**, 2721 (1979).
- ²J. Kwo and T. H. Geballe, *Phys. Rev. B* **23**, 3230 (1981); J. Kwo and T. H. Geballe, in Proceedings of the XVIth International Conference on Low Temperature Physics [*Physica* **108B&C**, 1665 (1982)].
- ³K. E. Kihlstrom and T. H. Geballe, *Phys. Rev. B* **24**, 4101 (1981).
- ⁴S. J. Bending, R. H. Hammond, and M. R. Beasley, *Bull. Am. Phys. Soc.* **29**, 385 (1984).
- ⁵J. M. Rowell and P. H. Schmidt, *Appl. Phys. Lett.* **29**, 622 (1976); J. M. Rowell, P. H. Schmidt, E. G. Spencer, P. D. Dernier, and D. C. Joy, *IEEE Trans. Magn.* **MAG-13**, 644 (1977).
- ⁶For a review of superconducting tunneling spectroscopy, see E. L. Wolfe, *Rep. Prog. Phys.* **41**, 1439 (1978).
- ⁷E. L. Wolf, J. Zasadzinski, G. B. Arnold, D. F. Moore, J. M. Rowell, and M. R. Beasley, *Phys. Rev. B* **22**, 1214 (1980).
- ⁸R. H. Hammond, *IEEE Trans. Magn.* **MAG-11**, 210 (1975); R. H. Hammond, *J. Vac. Sci. Technol.* **15**, 382 (1978).
- ⁹D. A. Rudman and M. R. Beasley, *Appl. Phys. Lett.* **36**, 1010 (1980).
- ¹⁰D. A. Rudman, F. Hellman, R. H. Hammond, and M. R. Beasley, *J. Appl. Phys.* **55**, 3544 (1984).
- ¹¹D. A. Rudman, Ph.D. thesis, Stanford University, 1982.
- ¹²F. Hellman, D. A. Rudman, R. H. Hammond, and T. H. Geballe, *Bull. Am. Phys. Soc.* **28**, 262 (1983).
- ¹³F. Hellman and T. H. Geballe, *Bull. Am. Phys. Soc.* **29**, 385 (1984).
- ¹⁴J. G. Adler and J. E. Jackson, *Rev. Sci. Instrum.* **37**, 1049 (1966).
- ¹⁵W. L. McMillan and J. M. Rowell, in *Superconductivity*, edited by R. D. Parks (Dekker, New York, 1969), Vol. 1, p. 561.
- ¹⁶J. Bostock, V. Diadiuk, W. N. Cheung, K. H. Lo, R. M. Rose, and M. L. A. MacVicar, *Phys. Rev. Lett.* **36**, 603 (1976).
- ¹⁷E. L. Wolf, J. Zasadzinski, J. W. Osmun, and G. B. Arnold, *J. Low Temp. Phys.* **40**, 19 (1980).
- ¹⁸G. B. Arnold, *Phys. Rev. B* **18**, 1076 (1978).
- ¹⁹The proximity parameters R and d/l are given by Eqs. (16) and (20) in Ref. 17.
- ²⁰H. Ihara, *Phys. Rev.* **27**, 551 (1983); Proceedings of the International Cryogenic Materials Conference, 1983, Colorado Springs (in press).
- ²¹J. Kwo, T. P. Orlando, and M. R. Beasley, *Phys. Rev. B* **24**, 2506 (1981).
- ²²T. P. Orlando, E. J. McNiff, Jr., S. Foner, and M. R. Beasley, *Phys. Rev. B* **19**, 4545 (1979).
- ²³B. P. Schweiss, B. Renker, E. Schneider, and W. Reichardt, in *Superconductivity in d- and f-band Metals*, edited by D. H. Douglass (Plenum, New York, 1976), p. 189.
- ²⁴J. Appel and W. Kohn, *Phys. Rev. B* **12**, 2682 (1975).
- ²⁵G. Bergmann and D. Rainer, *Z. Phys.* **263**, 58 (1973).
- ²⁶B. Mitrovic, C. R. Leavens, and J. P. Carbotte, *Phys. Rev. B* **21**, 5048 (1980).
- ²⁷P. B. Allen and R. C. Dynes, *Phys. Rev. B* **12**, 905 (1975). See Eqs. (13) and (22).
- ²⁸P. W. Anderson, K. A. Mullalib, and T. V. Ramakrishnan, *Phys. Rev. B* **28**, 117 (1983).